BEOL Embedded RF-MEMS Switch for mm-Wave Applications

M. Kaynak, K. E. Ehwald, J. Drews, R. Scholz, F. Korndörfer, D. Knoll, B. Tillack, R. Barth, M. Birkholz, K. Schulz, Y. M. Sun, D. Wolansky, S. Leidich[1], S. Kurth[1], Y. Gurbuz[2]

IHP, Im Technologiepark 25, 15236 Frankfurt (Oder), Germany
Tel: (+49) 335 5625 707, Fax: (+49) 335 5625 327, Email: kaynak@ihp-microelectronics.com
[1]Fraunhofer Research Institution for Electronic Nano Systems, 09126 Chemnitz, Germany
[2]Sabanci University Orhanli, 34956 Tuzla, Istanbul, Turkey

Abstract

We demonstrate for the first time the embedded integration of a Radio Frequency Microelectromechanical Systems (RF-MEMS) capacitive switch for mm-wave integrated circuits in a BiCMOS Back-end-of-line (BEOL). The switch shows state-of-the-art performance parameters. The "off" to "on" capacitance ratio is 1:10 providing excellent isolation in the mm-wave frequency range. Insertion loss and isolation are found to fall below 1.65dB and to exceed 15dB, respectively, in the frequency range of 60GHz to 110GHz. Feasibility of switch integration into single chip RF designs is demonstrated for a dual-band voltage controlled oscillator (VCO). No performance degradation was observed after ten billion hot-switching cycles.

Introduction

Latest developments in RF-MEMS technology have paved the way for achieving high performance, monolithically integrated structures, especially RF-MEMS switches (1, 2). Low insertion loss, high isolation, high linearity, near zero DC power consumption, and low cost of RF-MEMS switches are the most attractive features for RF circuit designers. Such switches are considered as the key components for next generation multi-band communication circuits (3, 4). Several methods were suggested to integrate MEMS components into IC using hybrid, monolithic, and post-processing techniques (5-9). Embedded MEMS switch integration into a standard CMOS or BiCMOS BEOL, as the most promising approach, has already been proposed by simulations (10), but was not successfully realized so far (11). Here, we demonstrate for the first time the embedded integration of an RF-MEMS capacitive switch for mm-wave integrated circuits in a BiCMOS BEOL. The integration is very simple, i.e. low-cost, adding only one mask step and a wet etch step to the BiCMOS baseline process. The switch shows state-of-the-art performance parameters. The "off" to "on" capacitance ratio is 1:10 providing excellent isolation in the mm-wave frequency range. Insertion loss and isolation are found to fall below 1.65dB and to exceed 15dB, respectively, in the frequency range of 60GHz to 110GHz. Typical switching on and off times are 20µs and 25µs, respectively, applying 30V actuation voltage. No performance degradation was observed after ten billion switching cycles. As a proof of concept, a dual-band VCO was designed to show the feasibility of RF-MEMS switch integration into single chip RF designs.

Technology

Fig. 1 illustrates the embedded RF-MEMS switch integration in IHP's 0.25µm SiGe:C BiCMOS process. The capacitive switch is built between the Metal2 (M2) and Metal3 (M3) layers. High-voltage electrodes are formed using Metal1 (M1) while M2 is used as RF signal line. A thin Si_3N_4/TiN layer stack, which is part of the BiCMOS metal-insulator-metal capacitor, forms the switch contact region. This configuration creates a height difference between the high-voltage electrode and the signal line which serves simultaneously as a stopping layer for the switch membrane. The membrane is realized using a stress compensated Ti/TiN/AlCu/Ti/TiN M3 layer stack. Note that this stress compensation did not lead to a violation of the original M3 process specifications. An SEM view of the switch is shown in Fig. 2, while Fig. 3 demonstrates that the switch integration adds only one mask step, a wet etch step and a critical-point drying step to the 8-inch, BiCMOS baseline process.

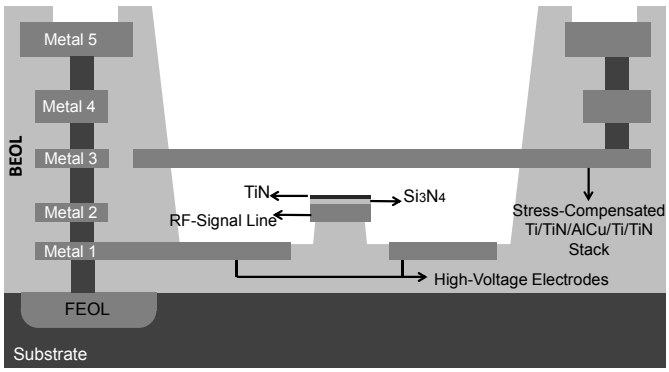

Fig. 1 Cross section of embedded RF-MEMS switch integration.

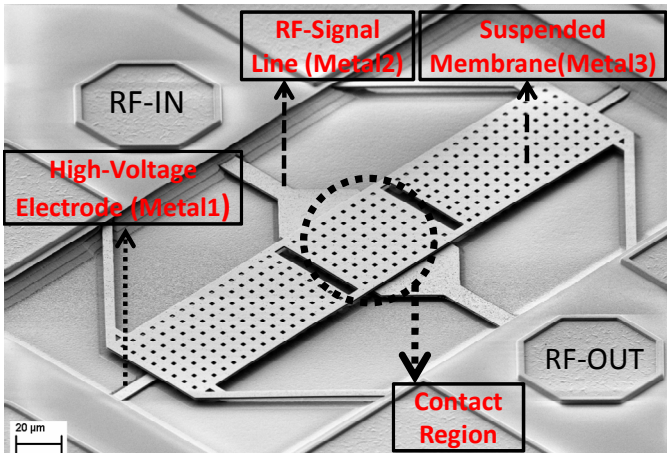

Fig. 2 SEM view of the RF-MEMS switch.

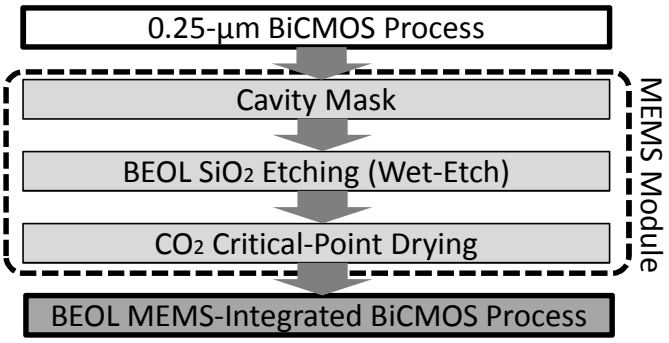

Fig. 3 Additional process steps for RF-MEMS switch integration into the BiCMOS process.

Results

Wafer-level measurements were done to characterize the switch performance. Fig. 4 shows the *C-V* characteristics of the switch for different sites on an 8-inch wafer. As can be seen, the pull-down voltage of the switch varies between 17V and 22V over the wafer due to a remaining M3 layer stress profile, resulting in a different initial gap between the high-voltage electrode and the membrane. The "off" state capacitance (membrane up) varies between 25fF and 30fF, while the "on" state (membrane down) ranges between 210fF and 250fF providing an *"off"/"on"* state capacitance ratio of at least 1:8, but typically 1:10. *S*-parameter measurement results are given in Fig. 5 for different sites of the wafer at 30V bias voltage. The insertion loss of the switch in the 1-110GHz frequency range is below 1.65dB. The isolation for frequencies between 60GHz and 100GHz is better than 15dB. S_{11} of the switch, given in Fig. 5 for the "off" state, demonstrates a good input matching to 50Ω. The resonance characteristic of the switch differs only by ±2GHz over an 8-inch wafer, as can be seen from Fig. 5 as well.

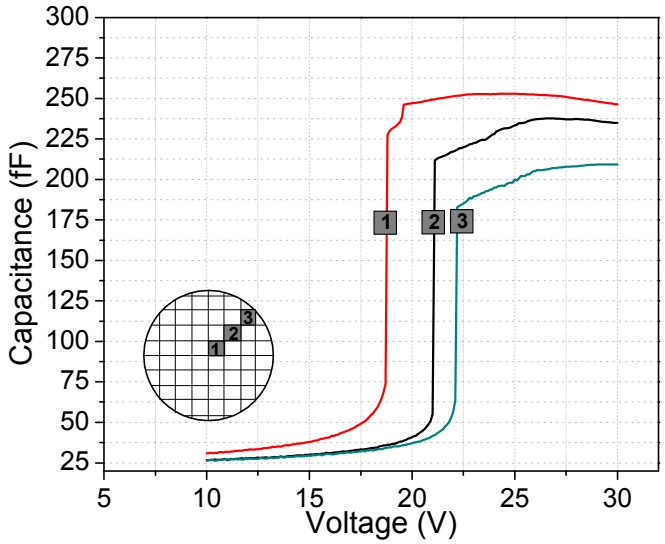

Fig. 4 Switch capacitance vs. voltage for three different sites on an 8-inch wafer.

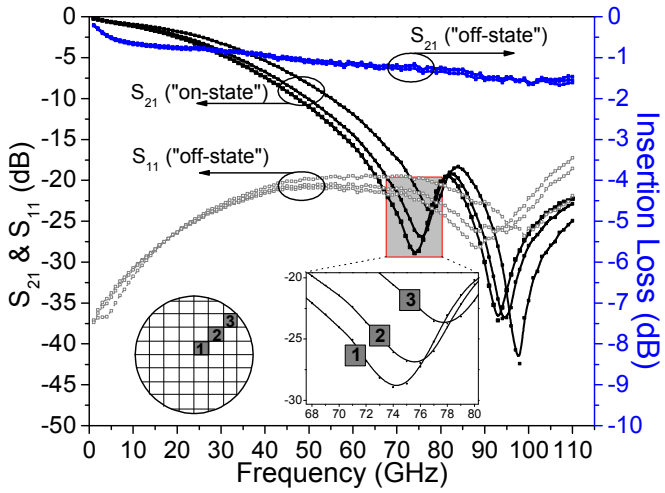

Fig. 5 S-parameters vs. frequency for switches on three different wafer sites. Insertion shows that the resonance frequency shifts from 74 GHz to 78 GHz due to "on-state" capacitance variation.

The switch dynamic behavior was characterized by time domain power measurements. The RF signal was up-converted to 100GHz and applied to the input of the switch, while the output was down-converted and observed in time domain using signal source analyzer. Fig. 6 shows the output power of the switch when a 30V pulse with a width of 50µs and a period of 10kHz was applied. From the same figure, 20µs switching time, 25µs releasing time, and 30dB isolation can be observed at 100 GHz.

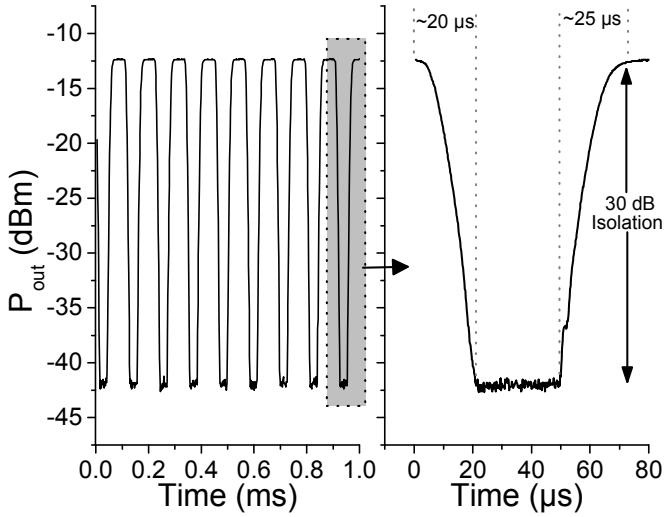

Fig. 6 Time-domain power measurements at 100 GHz. The left figure shows the output power at 10kHz pulse excitation and the right figure shows the switching-on and off times.

In addition to electrical measurements, the mechanical behavior of the switch was characterized by Laser-Doppler-Vibrometer (LDV). Fig. 7 shows the total *z*-displacement of the contact region versus time. A *z*-displacement of the switch membrane (gap between signal line and membrane) of 1.2µm can be observed from the same figure. A White-Light interferometer was used for topography characterization of the membrane before and after switching. Figs. 8a and 8b show the topography of the membrane in the "off" and "on" states. Fig. 8c shows the membrane displacement by calculating the local height difference between the initial "off" and the "on" position. The total *z*-displacement of the membrane at the center (indicated by white dashed line in Fig. 8c) is given in Fig. 8d. The deflection of 1.2µm at the contact region agrees well with the LDV measurement.

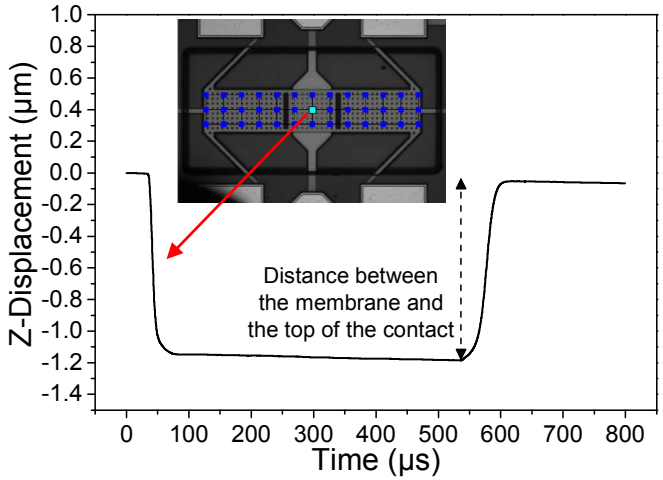

Fig. 7 *z*-displacement of one selected node (specified by green point) at 30V pulse actuation, measured by Laser-Doppler-Vibrometer.

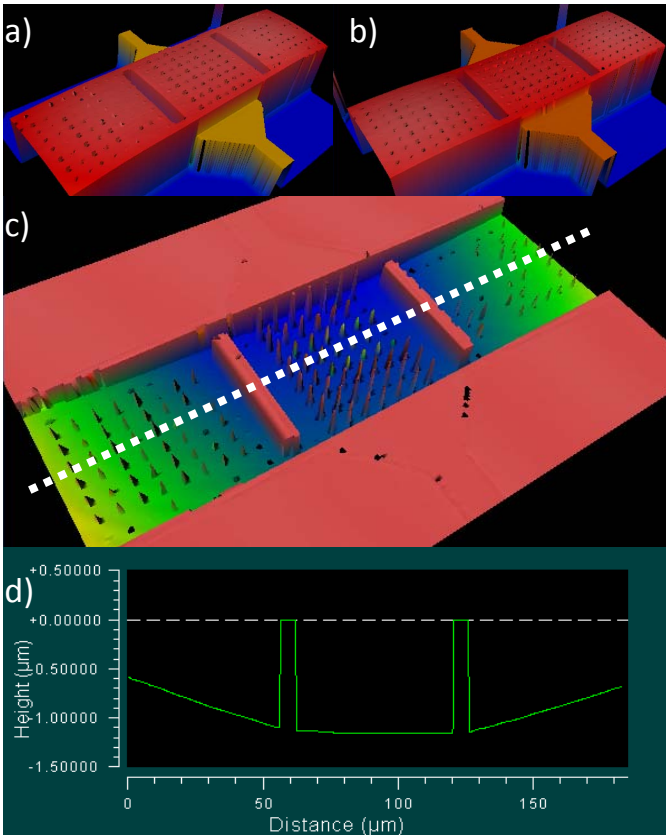

Fig. 8 White-Light Interferometer measurement results: a) "off-state" membrane topography, b) "on-state" membrane topography, c) displacement of membrane by taking the initial "off-state" position as reference, d) z-displacement of membrane (over the indicated white line on c). Middle part has z-displacement of 1.2 µm while sides have less to prevent from an electrical short between M1 and M3.

Design Example: Dual-Band VCO

As a proof of concept, a dual-band VCO was fabricated using the developed MEMS switch (Fig. 9).

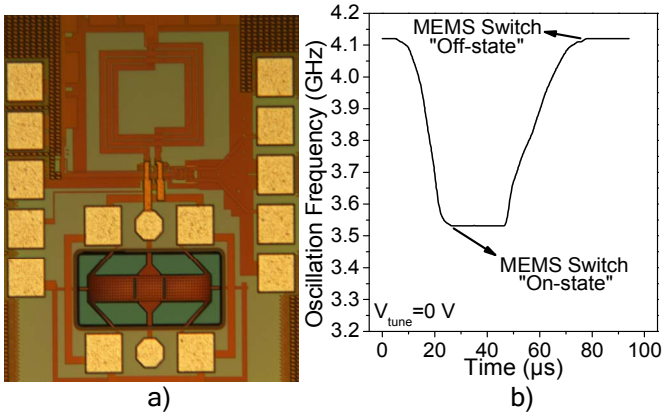

Fig. 9 a) Die photo of fabricated dual-band LC-VCO; b) Change of the oscillator frequency at a 30V step excitation with 50µs pulse width. The peak-to-peak RF-signal amplitude was 5V.

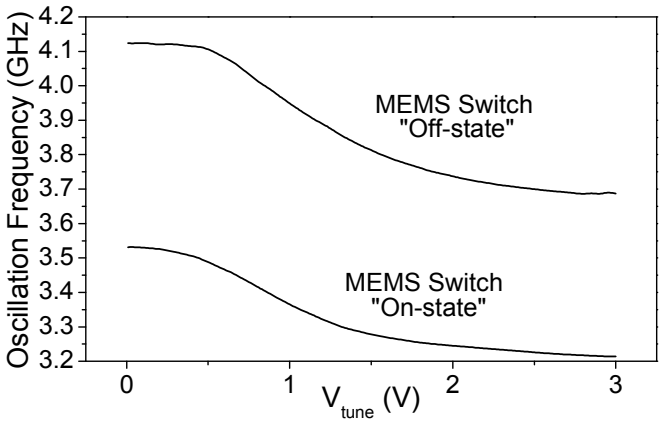

Fig. 10 Tuning characteristics of dual-band LC-VCO. Continuous frequency tuning is achieved by using a MOS varactor for both states.

The high capacitance ratio of 1:10 allows us to switch the oscillation frequency at 0V tuning voltage from 3.55 GHz to 4.15 GHz. Fig. 10 shows the VCO tuning behavior. Fig. 11 shows the output response of the VCO after a different number of hot-switching cycles under 5V peak-to-peak RF signal on the signal line of the switch. Fig. 12 shows the result of a preliminary life-time test of a standalone switch measured at ambient atmosphere. No performance degradation can be observed even after 5 billion switching cycles.

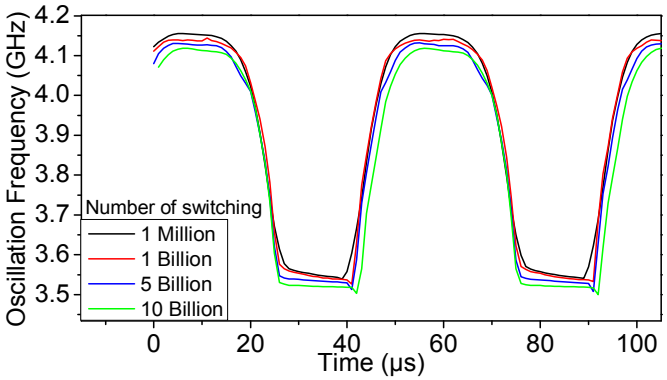

Fig. 11 Reliability test of the switch: Output frequency response of VCO after different number of switching cycles.

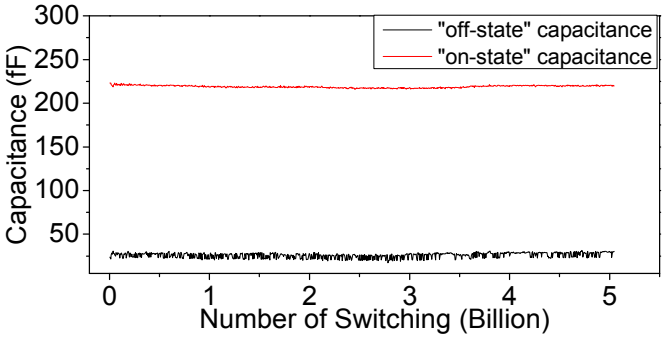

Fig. 12 Life-time test of standalone switch under 30V, 20kHz pulse.

Summary

Embedded BEOL integrated RF-MEMS capacitive switches for mm-wave IC applications have been successfully demonstrated. The BiCMOS process flow is extended by only one mask and an etch step. Over 10 billion operations are possible from the results of first life-time measurements. The high reproducibility and reliability of the developed technology makes the presented RF-switch feasible as a key component for reconfigurable circuits, such as matching networks, filters, antennas, phase-shifters and for the realization of single-chip high-performance, multi-band silicon RFICs.

Acknowledgements

The authors thank to the team of the IHP pilot line for excellent support, J. Borngräber for RF measurements and J. Katzer for SEM analysis.

References

(1) T.-J. King, et al., "Recent progress in modularly integrated MEMS technologies," *IEDM Tech. Dig.,* pp. 199-202, 2002 .

(2) Lingpeng Guan; Sin, J.K.O.; Haitao Liu; Zhibin Xiong, "Fully integrated CMOS and high voltage compatible RF MEMS technology," *IEDM Tech. Dig.*, pp. 35-38, 2004.

(3) Brown, E.R., "RF-MEMS switches for reconfigurable integrated circuits," *Microwave Theory and Techniques, IEEE Transactions on*, vol.46, no.11, pp.1868-1880, 1998.

(4) Rebeiz, G.M.; Muldavin, J.B., "RF MEMS switches and switch circuits," *Microwave Magazine, IEEE* , vol.2, no.4, pp.59-71, 2001.

(5) Tilmans, H.A.C., et al., "Wafer-level packaged RF-MEMS switches fabricated in a CMOS fab," *IEDM Tech. Dig.,* pp.41.4.1-41.4.4, 2001.

(6) Zhang, Q.X., et al., "Novel Monolithic Integration of RF-MEMS Switch with CMOS-IC on Organic Substrate for Compact RF System," *IEDM Tech. Dig.,* pp.1-4, 2006.

(7) Kuwabara, K., et al., "RF CMOS-MEMS Switch with Low-Voltage Operation for Single-Chip RF LSIs," *IEDM Tech. Dig.,* pp.1-4, 2006.

(8) Kawakubo, T.; Nagano, T.; Nishigaki, M.; Itaya, K., "High Reproducibility and Reliability of Piezoelectric MEMS Tunable Capacitors for Reconfigurable RF Front-end," *IEDM Tech. Dig.,* pp.435-438, 2007.

(9) Lei Gu; Xinxin Li, "Variable Capacitors and Tunable LC-Tanks Formed by CMOS-Compatible Metal MEMS for RF ICs," *IEDM Tech. Dig.,* pp.427-430, 2007.

(10) Guoan Wang; Hanyi Ding; Woods, W.; Mina, E., "Wideband on-chip RF MEMS switches in a BiCMOS technology for 60 GHz applications," *ICMMT Tech. Dig.,* pp.1389-1392, 2008.

(11) International Technology Roadmap for Semiconductors (ITRS), (http://public.itrs.net/).